Spectrum of Engineering Sciences
ISSN (e) 3007-3138 (p) 3007-312X Volume 4, Issue 3, 2026

GREEN SYNTHESIS CHARACTERIZATION AND ANTIMICROBIAL ACTIVITIES OF SILVER NANOPARTICLES USING LEAVES EXTRACT OF PROSOPIS CINERARIA

[1]Muhammad Shoaib, [2]Amam Laraib, [*3]Muhammad Iqbal, [4]Muhammad Akram
[1-3]Department of Chemical and Life Sciences, Qurtuba University of Science & Information Technology, Dera Ismail Khan, KP, Pakistan.
[4]Principal Scientific Officer, PCSIR Laboratories Complex, Peshawar, KP, Pakistan.
[1]shoaibramzan390@gmail.com, [2]anamlaraib8@gmail.com, [*3]drmuhammadiqbal@qurtuba.edu.pk, [4]drakrampcsir@gmail.com

Keywords
Prosopis cineraria, nickel oxide, nanoparticles, green synthesis, Salmonella typhi, Bacillus subtilis

Article History
Received on 14 Feb, 2026
Accepted on 10 March, 2026
Published on 12 March, 2026

Corresponding Author:
Muhammad Iqbal

Abstract
Present work represents ecofriendly green approach for the synthesis of silver nanoparticles using leaf extract of Prosopis cineraria and salt solution of silver nitrate. The synthesized nanoparticles were characterized using ultraviolet visible (UV-Vis), Fourier transform infrared (FT-IR), X-Rays diffraction (XRD) crystalline nature of silver nanoparticles and calculated size was 25 nm, high-resolution transmission electron microscopy (HRTEM), and scanning electron microscopy (SEM). techniques. High-resolution transmission electron microscopic analysis substantiated that the AgNPs were rod-shaped with an average size of 38 nm. SEM analysis revealed that the AgNPs were crystalline rod-shaped with porous morphology. Our SEM findings indicated that the size range of the produced silver nanoparticles exceeded the typical nanoparticle size range due to agglomeration, which should normally be between 25 to 28 nanometers. The proteins that surrounded and were bound to the surface of the produced silver nanoparticles caused their size range to be greater than the preferred size. X-ray diffraction study revealed that the AgNPs were in the face-centered cubic crystal system. The hydroxyl groups of Prosopis cineraria leaf extract acted as reducing agents, which was corroborated by the broad peak infrared spectrum 3400 cm-1. Peak at 3400-1 and a ester carbonyl peak near 1750 cm-1. The silver nanoparticles were confirmed by the presence of a very small peak 2300-1 of peaks along with two other peaks at 1615 cm-1 and 1320 cm-1. The antibacterial activities of silver nanoparticles inhibited the growth of bacterium that showed inhibition zone of 15 nm against Bacillus subtilis, and standard ciprofloxacin showed inhibition zone of 18 nm against the same bacterium. Salmonella typhi showed inhibition zone of 19 nm and standard drug ciprofloxacin showed inhibition zone of 21 nm against the same bacterium.

1. Introduction

An important application of nanotechnology is the manufacture of materials at nanoscale, their representation, manipulation, and application through the control of shape and size at the nanoscale. The preparation of nanoparticles is one of the most rapidly expanding domains of study in material science, and this field has been experiencing substantial growth worldwide. Depending on the characteristic size (1–100 nm), shape, and structure of the particles, nanoparticles exhibit entirely new or improved properties. There is increasing enthusiasm for gold and silver (noble metal) nanoparticles because they offer superior properties and useful flexibility. Silver nanoparticles have a substantial surface zone, resulting in remarkable biochemical, catalytic, and atomic reactivity compared to larger particles with the same chemical composition (Rafique *et al.*, 2017). Green chemistry concepts used in the biobased methodology for the synthesis of nanometals make it non-polluting, economically sustainable, and easy to scale up for large-scale manufacturing as compared to chemical methods that are often expensive, use dangerous chemicals, and are comparatively complicated (Singh *et al.*, 2018). Therefore, in the last several decades, nanotechnology has focused on the production of nanoparticles utilizing biological agents, such as plant extracts or microorganisms. The green synthesis process typically entails three key steps: choosing a reaction medium, choosing a bioreducing agent, and choosing non-carcinogenic materials to stabilize nanoparticles. However, because cell culture maintenance processes can be skipped and plant-mediated nanoparticle manufacturing can be done on a large scale in a non-sterile environment, it may be preferable to alternative biobased synthesis methods (Keat *et al.*, 2015)

Although nanoparticles are thought to be a modern scientific development, nanotechnology has been used for thousands of years. Dichroic glass, a peculiar variety of glass, was used to make the cup which produced amazing colors when light fall on it, which is kept in the British Museum in London. Another prominent use of simple nanotechnology is ruby red, which can be found as evidence in many old churches. It was used in stained-glass windows during the Middle Ages. Faraday produced the first gold nanoparticles, which were preserved at the Royal Institution in London (Ijaz *et al.*, 2020).

Silver nanoparticles (AgNPs) have attracted much attention from scientists recently because of their extraordinary potential against various drug-resistant bacteria (Geoprincy *et al.*, 2013; Maaz, 2018). Silver nanoparticles exhibit anti-inflammatory and antibacterial properties and expedite wound healing; consequently, they have been incorporated into pharmaceutical preparations, coatings for medical implants, and readily accessible wound dressings (Shah *et al.*, 2015; Katas *et al.*, 2018). These possess catalytic ability and have been used as catalysts in many processes (Lade & Patil, 2022). Owing to their unique characteristics, AgNPs are now used in various industries, including biomedical drug delivery, agriculture (Remya *et al.*, 2022) and water treatment (Chen *et al.*, 2018; Ragam & Mathew, 2020). Their high conductivity make them suitable for use in the preparation of pastes, electronics, adhesives, inks, and other products. Physiochemical techniques, such as chemical reduction, electrochemical procedures, microemulsions, laser ablation, gamma radiation, microwaves, and photochemical reduction, have

been used to produce AgNPs. These techniques offer effective production; however, they have drawbacks, such as the use of hazardous chemicals, high operating costs, and energy requirements. A low-cost and energy-efficient green technique is an alternative to physiochemical methods for the preparation of AgNPs and employs microorganisms, plant extracts, and organic polymers as reducing and capping agents (Ramya & Subapriya, 2012; Roy & Das, 2015).

Prosopis cineraria (L) Druce (Mesquite) is commonly known as Jand a perineal tree of family Fabaceae. It is naturally found in the dry and arid regions of Arabia, Afghanistan, India, Iran, and Pakistan. It provides shade and fodder and has wood that improves the soil and stabilizes sand dunes. It is commonly used in dryland agroforestry in India and Pakistan. It is a slow-growing tree species. It is a slow-growing tree species affected by water scarcity, erratic rainfall, and temperature extremes in desert conditions. Unlike other trees, *P. cineraria* produces lush green leaves during the hot summer season, which is a major source of fodder for livestock in the region. The leaves contain 18% calcium, 13.8%crude protein, and 20% crude fiber. *P. cineraria* provide magnificent firewood (calorific value, approximately 5000 Kcal/kg) and charcoal. The plant is a rich source of phenolics, flavonoids, steroids and tennis. These phytochemicals for necessary for synthesis and stabilization of nanoparticles (Pandey et al., 2023).

Silver Nanoparticles' Potentially Harmful Side Effects

Silver nano particles may have some negative impacts both on health and environment. Many industries, including those in the food, healthcare, cleaning, electronics, home appliances, toys, and medical equipment sectors, frequently use silver NPs. The physicochemical properties of silver NPs contribute to their potential toxicity, both in vivo and in vitro. Another environmental concern arises from the release of silver NPs, which can be readily absorbed by aquatic species, leading to toxic effects. Furthermore, the extensive use of silver NPs as a disinfectant poses a risk of microbial resistance, limiting its effectiveness (Saadh, 2021).

Materials and Methods

Research area

This research was conducted in the research laboratory of the Department of Chemical and Life Sciences, Qurtaba University, D.I. Khan. Khan.

Materials

The research involved the utilization of various materials, including chemicals and equipment, to facilitate experimental work. The chemicals used in this study were carefully selected to ensure the accuracy and reliability of the experiments. These included silver nitrate salt (Sigma Aldrich) for specific chemical reactions. Nutrient Agar (Linofilchem) was used as a growth medium for bacterial cultures. Distilled water (Manahil Enterprises) was used to prepare solutions and maintain consistency. Bacterial strains (Sigma Aldrich) were used as test organisms in microbiological assays. Prosopis cineraria leaves, Prosopis cineraria leaf powder, and Prosopis cineraria leaf extract were essential components for specific plant-based experiments. The experiments required a range of specialized equipment to effectively perform various procedures. These included aluminum foil (Basic U.A.E) for wrapping and sealing purposes. A magnetic hot plate (Jiangsu Jinyi Instrument Technology Company Limited) was used to control and maintain the temperature during the reactions. A cup borer (HT Star) was used to cut the uniform samples. Beakers (Iwaki TE-32 Asahi Glass) were used for measuring and mixing the solutions. Pipettes (Bomax) for accurate

liquid handling. Petri dishes (Sigma-Aldrich) were used for bacterial culture and growth. Conical flasks (Bomax) were used for mixing and storing the solutions. Micropipettes (Q pipettes) for precise microvolume measurements. Para Film (Bemis) for sealing containers and preventing contamination. A laminar flow hood (Kenton) provided a sterile environment for the sensitive experiments. The meticulous choice of these materials, encompassing both chemicals and equipment, played a pivotal role in ensuring the effective implementation of the research and enhancing the dependability and precision of the experimental outcomes.

Collection of *Prosopis Cineraria*

The leaves of the plant were collected near the village Kundiyan of district Mianwali and identified by a botanist.

Synthesis of *Prosopis Cineraria* Leaves Extract

Fresh leaves of *P. cineraria* were thoroughly washed with water to eliminate any dust or other contaminants and then shade-dried before being ground into a powder. Leaf extract was prepared by mixing 5 g of P. cineraria leaf powder with 100 mL of distilled water in a beaker with a capacity of 250 mL and slowly heating for a few minutes and magnetic stirring for 3 h on a magnetic hot plate. The resulting solution was filtered using Whatman filter paper (Ali *et al.*, 2016).

Preparation of Silver Nitrate Solution

Subsequently, 0.6 mM $AgNO_3$ was dissolved in 50 mL distilled water while being vigorously stirred at room temperature for approximately 15 min to produce 12 mM $AgNO_3$ (Kwon *et al.*, 2005).

Silver Nanoparticles Synthesis

A beaker (250 mL) was filled with 50 mL of aqueous $AgNO_3$ (12 mM) and 30 mL of leaf extract for a typical synthesis. The sample was then heated to 30 °C for a few minutes while being continuously stirred on a hot plate magnetic stirrer for 48 h. The color of the solution began to change within 5 min, from faded yellow to blackish brown (Kumar *et al.*, 2014).

Characterization of Silver Nanoparticles

To investigate the physical properties of silver nanoparticles, the following analyses were performed.

Fourier Transform Infrared Spectroscopy (FT-IR)

FT-IR spectra of leaf extract and the synthesized sliver nanoparticles were procured on Brucker FT-IR Tensor 27 Model between 4000-400 cm^{-1} (Kumar *et al.*, 2014)

X-Ray Diffraction (XRD)

For phase identification of the nanoparticles, X-ray diffraction (XRD) analysis was performed at 40 kV and 40 mA using CuKα radiation filtered with Ni-crystal monochromator. Powder X-ray diffraction (XRD) measurements were carried out using a multipurpose X-ray diffractometer (Bruker-AXS D8 Discover). The Gobel mirror forms a parallel beam diverging 0.03° The intensity of reflected beam was measured by LYNXEYE position sensitive detector (PSDC, Angular Resolution of 0.015°). Reflections were indexed using WinXPOW and PowderCell (Titus *et al.*, 2019)

High-Resolution Transmission Electron Microscopy (HRTEM)

High-resolution transmission electron microscopy (HRTEM) is used to observe the atomic-level crystallographic structure of a sample. In contrast to traditional microscopy, HR-TEM generates images based on interference in the image plane rather than absorption. Through the imaging system, where phase changes occur and interfere with each other, electrons interact separately with the sample. The recorded image does not accurately depict the true structure of the sample. However, owing to its superior resolution, this method is incredibly useful for investigating the

characteristics of materials at the nanoscale. It allows for the visualization of crystal structures, detection of crystallographic flaws, and even the study of single atoms (Titus *et al.*, 2019).

To investigate using high-resolution transmission electron microscopy (HRTEM), the synthesized nanoparticle solution was diluted. A small quantity of the diluted solution was applied separately to an aluminum foil and a carbon grid, and these surfaces were allowed to dry to assist in the analysis. An FEI TECNAI G2 system was used to conduct the HRTEM study (Venkatesan *et al.*, 2014).

Scanning Electron Microscopy (SEM)

Scanning electron microscopy of the synthesized silver nanoparticles was conducted on Hitachi S-3400N SEM instrument following reported protocol (Mohammed & Abdullah, 2018; (Anuradha *et al.*, 2011).

Antibacterial Activity of Silver Nanoparticles

Agar Well Diffusion Method

The antibacterial effectiveness of the AgNPs was assessed using the agar well diffusion technique. Throughout this procedure, the researchers took precautions to prevent bacterial contamination by wearing surgical gloves, face masks, and laboratory coats. The researcher systematically divided the process into distinct steps to gain a comprehensive understanding of each step (Periyasamy et al., 2018).

Sterilization of all Equipment Used in Antimicrobial Activity

All equipment, including Petri dishes, cup borer, teasing needles, beakers, conical flasks, micropipette tips, and cotton swabs, were sterilized using a 35-min steam autoclaving process. Subsequently, the sterilized items were transferred to a laminar flow hood. Before placement in the laminar flow hood, the UV lamp was activated for 5 min. After this initial period, the UV lamp was turned off, but the hood light and fan remained operational (Periyasamy et al., 2018).

Preparation of Agar Solution

A 7.5 g portion of nutrient agar ISO 16266 was dissolved in 150 mL distilled water and placed on a magnetic hot plate (78-I) for approximately 25 min, maintaining a temperature between 30°C and 40°C for 5 min while stirring. Subsequently, the prepared agar solution was subjected to steam autoclaving for approximately 20 min, removing from the machine when the pressure gauge indicated 1.7 bar. The agar solution was then poured into Petri dishes without allowing it to cool. The scholar observed that the agar did not solidify in the Petri dishes unless it had been adequately autoclaved. When removing the agar solution from the autoclave, it was important to ensure that it exhibited a concentrated, sticky consistency without direct contact, which could be discerned through visual observation (Periyasamy et al., 2018).

Solidification of Agar solution in Petri Dishes

Two Petri dishes were placed in a laminar flow hood, and 25 mL of the evaporating agar solution was gently poured into a designated area within each dish. The dishes were then left in the laminar flow hood for 40 min. Throughout this time, the hood's light and fan were operational, but the UV rays were switched off. After 40 min, a well-defined layer of agar solution formed within the Petri dishes, as shown in Figure 3.1.

Figure 1: Petri dish with nutrient ager layer placed in a laminar flow hood

Bacterial Inoculation

Once a solid layer of nutrient agar had formed in each Petri dish, bacteria were introduced onto the agar surface using sterilized cotton swabs in a zig-zag pattern to ensure that the entire circular area of the agar received thorough inoculation with the bacterial culture. Specifically, one Petri dish was inoculated with a Bacillus suspension, and the second Petri dish was inoculated with a suspension of Salmonella bacteria (Periyasamy et al., 2018).

Wells Formation on Agar Layer

Two wells were made at the corners of each Petri dish agar layer using a cup borer, as illustrated in Figure 3.2. If some agar remained at the well sites, it was carefully extracted using a cup borer. If any material persisted, a sterilized teasing needle was used to remove it.

Figure 2: Petri dish showing sells in agar layer

Insertion of Standard and Sample in Wells

Silver nanoparticle powder (0.5 g) and Ciprofloxacin (250 mg) were mixed with 10 mL of ampoule water (water intended for injection purposes). Similarly, silver nanoparticle powder (0.5 g) and Ciprofloxacin (250 mg) were mixed with 10 mL of ampoule water (water suitable for injection), as illustrated in Figure 3.3.

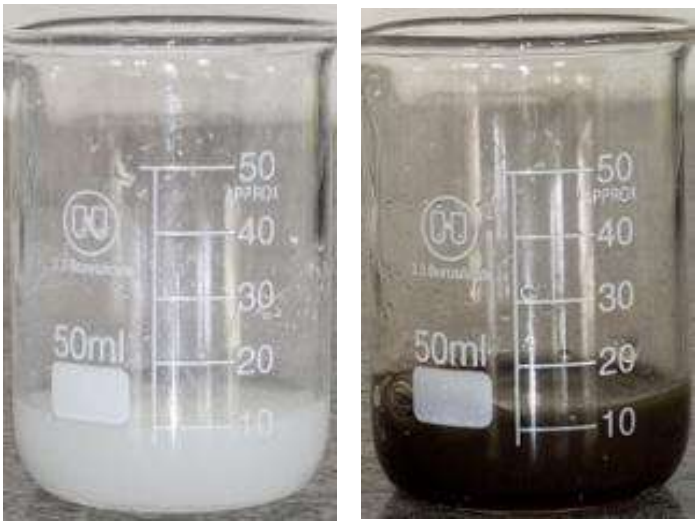

Figure 3: (A) 0.5 g Sample 10 ml Ampoule Water in Mixture (B) 250 mg Ciprofloxacin and 10 ml Ampoule Water

In each Petri dish, 28 µL of the sample solution was carefully added to one well, and 28 µL of the control ciprofloxacin solution was added to a separate well. Subsequently, the Petri dishes were sealed using Parafilm, which was marked with a black marker for identification, and then incubated in an oven set at a temperature of 30 °C. After a 24-h incubation period, an inhibition zone developed on the agar surface, and its size was measured using a millimeter scale.

Results and Discussions

This chapter describes every step undertaken to produce silver nanoparticles and characterize them using Fourier transform infrared spectroscopy, X-ray diffraction spectroscopy, high-resolution transmission electron microscopy, and scanning electron microscopy. It also presents the results of the antibacterial activity analysis. The findings of the analysis are as follows:

Color Change of Solution of Plant Extract and Silver Nitrate

Figure 4: Color change during the synthesis of silver nanoparticles. (A) Yellowish AgNPs of Prosopis cineraria at the start of the reaction. (B) Blackish-brown AgNPs of Prosopis cineraria at the start of the reaction.

The change in color from fade yellow to blackish brown indicates that *Prosopis cineraria* leaf extract was successfully used to synthesize silver nanoparticles. In another study, *Bryophyllum pinnatum* plant extract was used for the synthesis of silver nanoparticles, and the appearance of a dark brown color confirms the synthesis of silver nanoparticles. Metal nanoparticles are responsible for these distinctive color differences (Baishya *et al.*, 2012).

Characterization Analysis

The following techniques were used to characterize the silver nanoparticles.

FTIR Analysis of AgNPs

Fourier-transform infrared (FT-IR) spectroscopy was used to analyze the chemical composition of P. cineraria leaf extract. The band observed at 3400 cm^{-1} is attributed to the stretching vibrations of various functional groups. This technique helps identify the specific chemical constituents present in the extract. These variations in bands are attributed to the stretching vibrations in alcohols, phenols, and carboxylic acids. Different molecules and their surroundings can slightly shift the absorption frequency; however, the general range indicates the presence of OH groups. The FT-IR band observed at 3090 cm^{-1} is associated with C-H stretching vibrations, particularly in saturated hydrocarbons. The bands observed at 2910 cm^{-1} and 2851 cm^{-1} correspond to stretching vibrations in aliphatic hydrocarbons, specifically, symmetric and asymmetric stretching of CH_2 and CH_3 groups, respectively. The band observed at 1815 cm^{-1} indicates a carbonyl group conjugated with a double bond or an aromatic ring. The band observed at 1750 cm^{-1} signifies a carbonyl group, commonly found in compounds such as aldehydes, ketones, carboxylic acids, and esters. The bands observed at 1615 cm^{-1}, 1460 cm^{-1}, and 1410 cm^{-1} correspond to C=C stretching in aromatic compounds, CH_2 bending in aliphatic compounds, and the presence of the methylene group, respectively. The band observed at 1320 cm − 1 indicates the presence of CH_3 groups. The band observed at 1270 cm^{-1} suggests the stretching vibration of C-O bonds. Furthermore, the band observed at 1190 cm^{-1} is characteristic of compounds with amine groups. The band observed at 1050 cm^{-1} represents C-N stretching vibrations, typically found in compounds containing carbon and nitrogen. The band observed at 930 cm^{-1} indicates aromatic C-H bending vibrations, often observed in molecules with benzene rings. The bands observed at 810 cm^{-1} and 790 cm^{-1} are related to out-of-plane bending vibrations in aromatic rings. The band observed at 600 cm^{-1} indicates hydrogen-bending vibrations in aromatic compounds. Therefore, in *P. cineraria* leaf extract, AgNPs were found in the range of 290–490 cm^{-1}. It was also reported that AgNPs were found in the range of 290–490 cm^{-1} (Ruman & Kia, 2021).

It has also been reported that the O–H stretching vibration indicates the presence of hydroxyl groups, which play a role in reducing silver ions to form silver nanoparticles (Phatak & Hendre, 2015). Moreover, the presence of C=O bonds indicate the involvement of protein carbonyl groups, implying that proteins act as capping agents for silver nanoparticles. Proteins have a strong affinity for binding with silver nanoparticles, thereby imparting stability to these metal nanoparticles (Umoren *et al.*, 2014). FTIR analysis of the sample conclusively established the presence of organic molecules, such as carboxyl, hydroxyl, and amino groups, on the surface of the silver nanoparticles. This indicates that substances from plants are not only involved in the preparation of these

nanoparticles but also in maintaining their stability (Nayak *et al.*, 2021).

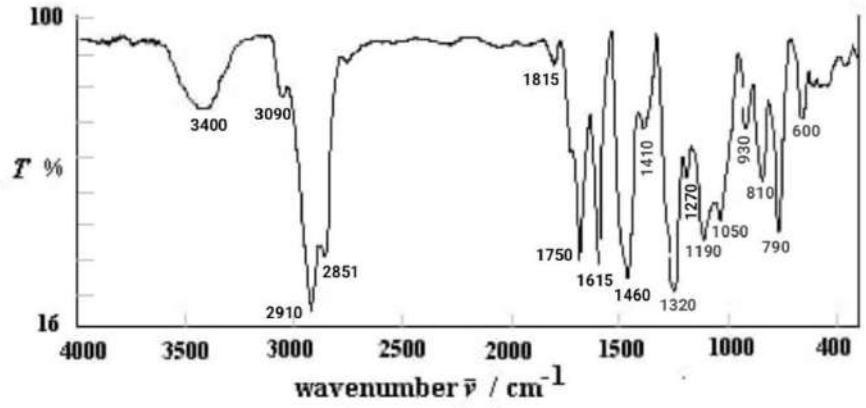

Figure 5: FTIR Spectrum of Silver Nanoparticles

XRD Analysis of AgNPs

X-ray diffraction (XRD) analysis served to ascertain the crystalline nature of the sample, offering more than just its identity. In cases involving mixtures, XRD patterns become a valuable tool for calculating the elemental ratios within the sample. Data analysis can provide further insights into the structural state of specific elements, their degree of crystallinity, and any deviations from their ideal compositions. When interacting with the atomic planes, only a fraction of the X-ray beam is transmitted, whereas the remainder is subjected to absorption, refraction, dispersion, and diffraction by the sample. The distinctive atomic composition and arrangement of each element results in varying patterns of X-ray diffraction (Titus *et al.*, 2019).

Diffraction intensities ranging from 20° to 80° were measured at 2θ angles. Strong peak values of 2θ have been seen at angles of 38.45°, 46.35°, 64.75°, and 78.05° have been observed (Figure 4.6). Similar peaks for silver nanoparticles were observed when they were synthesized using the leaf extract of *Urtica dioica Linn* (Jyoti et al., 2016). Diffraction intensities were compared and analyzed, and the results demonstrated that the synthesized silver nanoparticles had a face-centered cubic crystalline structure. The diffraction data were used to measure the crystallite size, which was found to be 25 nm. These findings matched the data in the Joint Committee on Powder Diffraction Standards (JCPDS) database, confirming the formation of AgNPs.

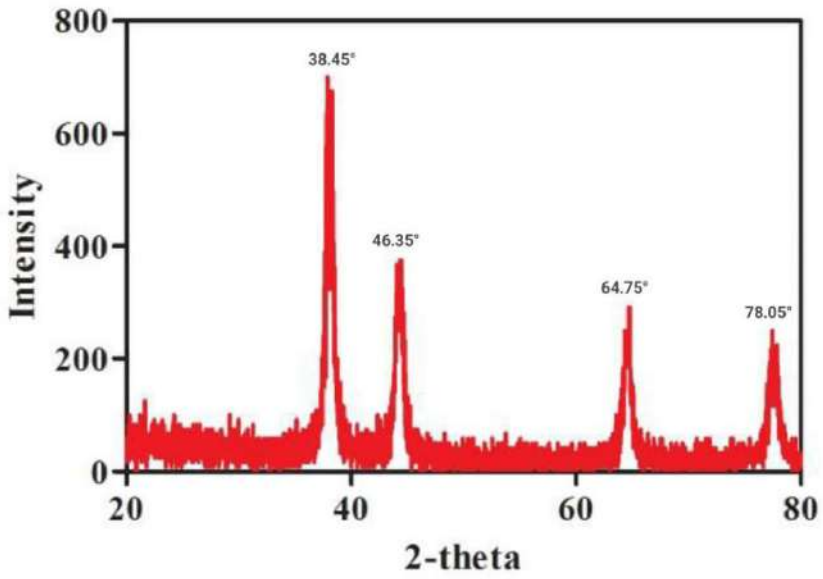

Figure 6: XRD Peak Diffractogram of Silver Nanoparticles

HRTEM Analysis of AgNPs

HR-TEM was used to gain insights into the morphology, size, and arrangement of AgNPs, and the results revealed finer aspects of their morphology (Bhat *et al.*, 2021). AgNPs were generally rod-shaped, with a consistent structure, as observed via HRTEM (Figure 4.8). The experimental results showed that the nanoparticles produced in the sample had calibrated sizes between 31 and 42 nm, with an average size of 38 nm. AgNPs with average particle sizes of 38 nm were produced using Prosopis cineraria leaf extracts. HR-TEM image analysis verified the production of silver nanoparticles. HR-TEM micrographs indicate that the particles were smaller 28 nm, a size smaller than 100 nm in size (Nayak *et al.*, 2021).

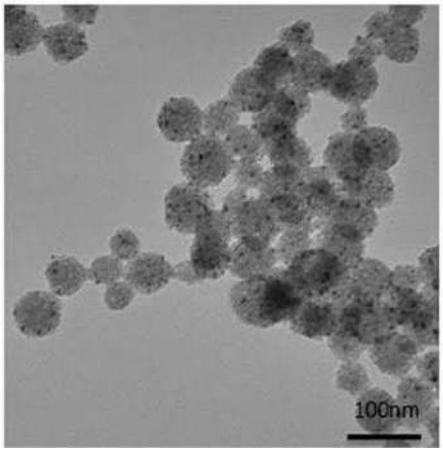

Figure 7: HRTEM Analysis of synthesized silver nanoparticles

SEM Analysis of AgNPs

Scanning electron microscopy (SEM) was used to determine the size and shape of the green-synthesized silver nanoparticles. The experimental results revealed that the nanoparticles produced in the sample show aggregation and porous morphology. Aggregated particles showed size larger than measured through HRTEM (28 nm) and XRD (25 nm). The calibrated sizes are between 134 and 271 nm, with an average size of 188 nm. Our findings indicate that the size range of the produced silver nanoparticles exceeded the typical nanoparticle size range, which should normally be between 1 and 100 nm. The proteins that surrounded and were bound to the surface of the produced silver nanoparticles caused their size range to be greater than the preferred size. Our findings correspond with the results reported by Mukherjee *et al.* The stabilization of cysteine-containing proteins in solution may be the cause of the stability of the nanoparticles (Maliszewska *et al.*, 2009). Literature on green synthesis of silver nanoparticles from leaf extracts of *Pinus densiflora*, *Diospyros kaki*, *Ginkgo biloba*, *Magnolia kobus*, *and Platanus orientalis* to show stable AgNPs with average sizes ranging from 15 to 500 nm (Chung *et al.*, 2016). The morphology of the AgNPs revealed rod-shaped particles. The SEM images also show significant agglomeration of silver nanoparticles at specific locations. This could be attributed to the magnetic properties of AgNPs and their high surface-area-to-volume ratio, which drives them to aggregate as a means of reducing surface energy (Prucek *et al.*, 2011).

In another study, the average size of green-synthesized silver nanoparticles using Prosopis cineraria leaf extract was reported to be 40–60 nm (Periyasamy *et al.*, 2018). Similarly, the shape and structure differ from those of nanoparticles produced using similar techniques (Tailor *et al.*, 2020).

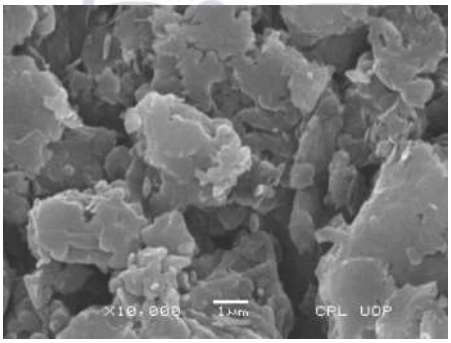

Figure 8: SEM Analysis of Synthesized Silver Nanoparticles

Antimicrobial Activity of AgNPs

After 24 h, the inhibition zones developed on the Petri dishes were measured in millimeters. The control (ciprofloxacin suspension) showed a maximum response against Bacillus, with an inhibition zone of 18 mm in diameter. The silver nanoparticle samples also showed a positive response against Bacillus, with an inhibition zone of 15 mm in diameter.

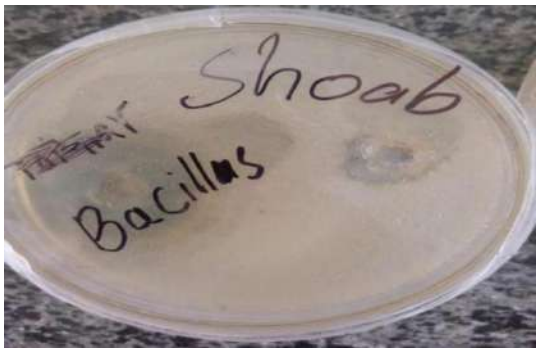

Figure 9: Antibacterial Activity of AgNPs against Gram Positive Bacterium Bacillus subtilis.

The control (ciprofloxacin suspension) showed an effective response against Salmonella, with an inhibition diameter of 21 mm. The silver nanoparticle sample showed a comparative response against Salmonella, with an inhibition zone diameter of 19 mm.

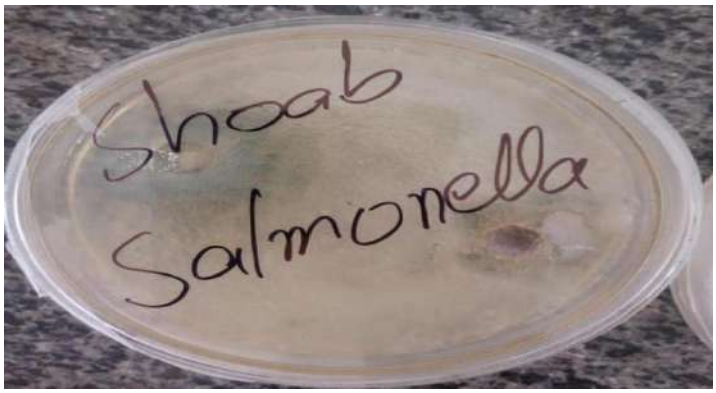

Figure 10: Antibacterial Activity of AgNPs against Gram Positive Bacterium Salmonellae typhi

Table 1: ***Antibacterial Inhibition zones synthesized silver nanoparticles against***

Sr. No.	**Names of bacteria**	**Control (Ciprofloxacin suspension)**	**AgNPs from *Prosopis cineraria***
1	*Bacillus subtilis*	18 mm	15 mm
2	*Salmonella typhi*	21 mm	19 mm

Our findings further showed that *Prosopis cineraria* AgNPs had potent antibacterial activity against Bacillus and Salmonella. However, the literature has shown that gram-negative bacteria (*Salmonella typhi*) are more susceptible to the bactericidal effects of nanoparticles than gram-positive (*Bacillus subtilis*) bacteria, because they have thicker peptidoglycan cell walls (Naveena & Prakash, 2013).

Conclusion

In this work we conducted an extensive investigation into the eco-friendly production of silver nanoparticles using *Prosopis cineraria* leaves and subsequently analyzed these nanoparticles for their unique attributes. Our findings affirm the practicality and effectiveness of harnessing *Prosopis cineraria* leaves as a sustainable resource for silver nanoparticles. This synthesis environmentally and

resulting nanoparticles exhibited desirable characteristics, such as precise size and shape, which were verified through diverse analytical techniques including SEM, HRTEM, and XRD. Additionally, Fourier-transform infrared (FTIR) analysis provided insights into the role of proteins in *Prosopis cineraria* leaves in stabilizing and capping these nanoparticles.

Notably, a significant discovery in our research was the remarkable antimicrobial effectiveness of these silver nanoparticles against gram-negative (*Salmonella typhi*) and gram-positive (*Bacillus subtilis*) bacteria. This antimicrobial potential suggests promising applications in various fields, including medicine, agriculture, and environmental restoration. In summary, our thesis not only advances the field of green nanoparticle synthesis but also underscores the substantial antimicrobial prowess of silver nanoparticles produced from *Prosopis cineraria* leaves. This environmentally considerate synthesis process and potent antimicrobial properties position these nanoparticles as valuable candidates for further investigation and potential deployment in combating microbial infections and related challenges.

Funding Source

No funding source

Conflict of Interest

Authors declare no conflict of interest.

References

Ahmed, R. H., & Mustafa, D. E. (2020). Green synthesis of silver nanoparticles mediated by traditionally used medicinal plants in Sudan. *International Nano Letters*, *10*(1), 1-14. https://doi.org/10.1007/s40089-019-00291-9

Ali, M., Kim, B., Belfield, K. D., Norman, D., Brennan, M., & Ali, G. S. (2016). Green synthesis and characterization of silver nanoparticles using Artemisia absinthium aqueous extract a comprehensive study. *Materials Science and Engineering: C*, *58*, 359-365.https://doi.org/10.1016/j.msec.2015.08.045

Anuradha, J., Abbasi, T., & Abbasi, S. A. (2011). Rapid and reproducible 'green'synthesis of silver nanoparticles of consistent shape and size using Azadirachta indica. *Research Journal of Biotechnology*, *6*(1), 69-70.

Baishya, D., Sharma, N., & Bora, R. (2012). Green synthesis of silver nanoparticle using Bryophyllum pinnatum (Lam.) and monitoring their antibacterial activities. *Archives of applied science research*, *4*(5), 2098-2104.

Bhat, M., Chakraborty, B., Kumar, R. S., Almansour, A. I., Arumugam, N., Kotresha, D., ... & Nayaka, S. (2021). Biogenic synthesis, characterization and antimicrobial activity of Ixora brachypoda (DC) leaf extract mediated silver nanoparticles. *Journal of King Saud University-Science*, *33*(2),101296. https://doi.org/10.1016/j.jksus.2020.101296

Chen, T., Shi, P., Zhang, J., Li, Y., Duan, T., Dai, L., ... & Zhu, W. (2018). Natural polymer konjac glucomannan mediated assembly of graphene oxide as versatile sponges for water pollution control. *Carbohydrate polymers*, *202*, 425-433.
https://doi.org/10.1016/j.carbpol.2018.08.133

Chung IM, Park I, KSH, Thiruvengadam M, Rajakumar G (2016). Plant-mediated synthesis of silver nanoparticles: their characteristic properties and therapeutic applications. *Nanoscale research letters*, *11*, 1-14. https://doi.org/10.1186/s11671-016-1257-4

Elemike, E. E., Onwudiwe, D. C., Arijeh, O., & Nwankwo, H. U. (2017). Plant-mediated

biosynthesis of silver nanoparticles by leaf extracts of Lasienthra africanum and a study of the influence of kinetic parameters. *Bulletin of Materials Science*, *40*, 129-137. https://doi.org/10.1007/s12034-017-1362-8

Geoprincy, G., Srri, B. V., Poonguzhali, U., Gandhi, N. N., & Renganathan, S. (2013). A review on green synthesis of silver nanoparticles. *Asian Journal of Pharmaceutical and clinical research*, *6*(1), 8-12.

Ijaz, I., Gilani, E., Nazir, A., & Bukhari, A. (2020). Detail review on chemical, physical and green synthesis, classification, characterizations and applications of nanoparticles. *Green Chemistry Letters and Reviews*, *13*(3), 223-245.

https://doi.org/10.1080/17518253.2020.1802517

Jyoti, K., Baunthiyal, M., & Singh, A. (2016). Characterization of silver nanoparticles synthesized using Urtica dioica Linn. leaves and their synergistic effects with antibiotics. *Journal of Radiation Research and Applied Sciences*, *9*(3), 217-227. https://doi.org/10.1016/j.jrras.2015.10.002

Katas, H., Moden, N. Z., Lim, C. S., Celesistinus, T., Chan, J. Y., Ganasan, P., & Suleman Ismail Abdalla, S. (2018). Biosynthesis and potential applications of silver and gold nanoparticles and their chitosan-based nanocomposites in nanomedicine. *Journal of Nanotechnology*, *2018*, 1-13. https://doi.org/10.1155/2018/4290705

Keat, C. L., Aziz, A., Eid, A. M., & Elmarzugi, N. A. (2015). Biosynthesis of nanoparticles and silver nanoparticles. *Bioresources and Bioprocessing*, *2*(1), 1-11. https://doi.org/10.1186/s40643-015-0076-2

Kumar, S., Singh, M., Halder, D., & Mitra, A. (2014). Mechanistic study of antibacterial activity of biologically synthesized silver nanocolloids. *Colloids and Surfaces A: Physicochemical and Engineering Aspects*, *449*, 82-86. https://doi.org/10.1016/j.colsurfa.2014.02.027

Kwon, J. W., Yoon, S. H., Lee, S. S., Seo, K. W., & Shim, I. W. (2005). Preparation of silver nanoparticles in cellulose acetate polymer and the reaction chemistry of silver complexes in the polymer. *Bulletin of the Korean Chemical Society*, *26*(5), 837-840. https://doi.org/10.5012/bkcs.2005.26.5.837

Lade, B., & Patil, A. (2022). Green synthesis and characterization of silver nanoparticles synthesized using leaf extract of passiflora foetida linn. *Journal of Sustainable Materials Processing and Management*, *2*(2) 57-68. https://doi.org/10.30880/jsmpm.2022.02.02.008

Maaz, K. (2018). Silver nanoparticles - fabrication, characterization and applications. In *InTech. eBooks*. https://doi.org/10.5772/intechopen.71247

Naveena, B. E., & Prakash, S. (2013). Biological synthesis of gold nanoparticles using marine algae Gracilaria corticata and its application as a potent antimicrobial and antioxidant agent. *Asian J Pharm Clin Res*, *6*(2), 179-182.

Nayak, S., Ghugare, P., & Vaidhun, B. (2021). Green-synthesis of Silver Nanoparticles by Hygrophila auriculata Extract: Innovative Technique and Comprehensive Evaluation. *Indian J. Pharm. Educ. Res*, *55*, S510-S517. https://doi.org/10.5530/ijper.55.2s.122

Pandey, V., Patel, S., Danai, P., Yadav, G., & Kumar, A. (2023). Phyto-constituents profiling of Prosopis cineraria and in vitro assessment

of antioxidant and anti-ulcerogenicity activities. *Phytomedicine Plus*, *3*(3), 100452. https://doi.org/10.1016/j.phyplu.2023.100452

Periyasamy, Y., Baskaran, B., Senniappan, V., & Chidambaram, S. (2018). Green synthesis and characterization of silver nanomaterials using leaf extract of Prosopis cineraria for antibacterial and anticancer applications. *Materials Research Express*, *5*(10), 105402. https://doi.org/10.1088/2053-1591/aadb4f

Phatak, R. S., & Hendre, A. S. (2015). Sunlight induced green synthesis of silver nanoparticles using sundried leaves extract of Kalanchoe pinnata and evaluation of its photocatalytic potential. *Der Pharmacia Lettre*, *7*(5), 313-324.

Prucek, R., Tuček, J., Kilianová, M., Panáček, A., Kvítek, L., Filip, J., ... & Zbořil, R. (2011). The targeted antibacterial and antifungal properties of magnetic nanocomposite of iron oxide and silver nanoparticles. *Biomaterials*, *32*(21), 4704-4713. https://doi.org/10.1016/j.biomaterials.2011.03.039

Rafique, M., Sadaf, I., Rafique, M. S., & Tahir, M. B. (2017). A review on green synthesis of silver nanoparticles and their applications. *Artificial cells, nanomedicine, and biotechnology*, *45*(7), 1272-1291. https://doi.org/10.1080/21691401.2016.1241792

Ragam, P. N., & Mathew, B. (2020). Unmodified silver nanoparticles for dual detection of dithiocarbamate fungicide and rapid degradation of water pollutants. *International Journal of Environmental Science and Technology*, *17*, 1739-1752. https://doi.org/10.1007/s13762-019-02454-9

Ramya, M., & Subapriya, M. S. (2012). Green synthesis of silver nanoparticles. *Int J Pharm Med Biol Sci*, *1*(1), 54-61.

Remya, R. R., Julius, A., Suman, T. Y., Aranganathan, L., Dhas, T. S., Mohanavel, V., ... & Muhibbullah, M. (2022). Biofabrication of silver nanoparticles and current research of its environmental applications. *Journal of Nanomaterials*, *2022*, 1-11. https://doi.org/10.1155/2022/2670429

Ruman, U., & Kia, P. (2021). Biosynthesis and Characterization of Silver Nanoparticles from Bitter Melon (Momordica charantia) Fruit and Seed Extract and their Antimicrobial Activity. *Journal of Research in Nanoscience and Nanotechnology*, *2*(1), 1-11. https://doi.org/10.37934/jrnn.2.1.111

Saadh, M. J. (2021). Synthesis, role in antibacterial, antiviral, and hazardous effects of silver nanoparticles. *Pharmacologyonline*, *2*, 1331-1336.

Shah, M., Fawcett, D., Sharma, S., Tripathy, S. K., & Poinern, G. E. J. (2015). Green synthesis of metallic nanoparticles via biological entities. *Materials*, *8*(11), 7278-7308. https://doi.org/10.3390/ma8115377

Singh, J., Dutta, T., Kim, K. H., Rawat, M., Samddar, P., & Kumar, P. (2018). 'Green'synthesis of metals and their oxide nanoparticles: applications for environmental remediation. *Journal of nanobiotechnology*, *16(1)* 1-24. https://doi.org/10.1186/s12951-018-0408-4

Singh, M., Sinha, I., & Mandal, R. K. (2009). Role of pH in the green synthesis of silver nanoparticles. *Materials Letters*, *63(3-4)*, 425-427. https://doi.org/10.1016/j.matlet.2008.10.067

Tailor, G., Yadav, B. L., Chaudhary, J., Joshi, M., & Suvalka, C. (2020). Green synthesis of silver nanoparticles using Ocimum canum and their antibacterial activity. *Biochemistry and Biophysics Reports*, *24*, 100848. https://doi.org/10.1016/j.bbrep.2020.100848

Titus, D., Samuel, E. J. J., & Roopan, S. M. (2019). Nanoparticle characterization techniques. In *Green synthesis, characterization and applications of nanoparticles* (pp. 303-319). Elsevier. https://doi.org/10.1016/B978-0-08-102579-6.00012-5

Umoren, S. A., Obot, I. B., & Gasem, Z. M. (2014). Green synthesis and characterization of silver nanoparticles using red apple (Malus domestica) fruit extract at room temperature. *J. Mater. Environ. Sci*, *5*(3), 907-914.

Venkatesan, B., Subramanian, V., Tumala, A., & Vellaichamy, E. (2014). Rapid synthesis of biocompatible silver nanoparticles using aqueous extract of Rosa damascena petals and evaluation of their anticancer activity. *Asian Pacific journal of tropical medicine*, *7*, S294-S300. https://doi.org/10.1016/S1995-7645(14)60249-2